

SPH Simulations of Barred Galaxies: Evolution of Nuclear Rings

H. B. ANN

Division of Science Education, Pusan National University, Pusan 609-735, Korea

E-mail: hbann@cosmos.es.pusan.ac.kr

(Received Sep. 29, 2001; Accepted Nov. 15, 2001)

ABSTRACT

Numerical simulations based on the smoothed particle hydrodynamics (SPH) is performed to investigate the dynamical properties of barred galaxies that have nuclear rings. The nuclear ring morphology depends on the relative strength of bar potentials. Nuclear rings form between the two ILRs and align perpendicular to the bars unless the bar potentials are strong enough to allow the x1 orbits near the ILRs. Shock dissipation plays a critical role in the formation of nuclear rings.

Key Words : methods: numerical — SPH

I. INTRODUCTION

Nuclear rings are powerful probes tackling the inner dynamics of galaxies. Recent high resolution images of the central regions of spiral galaxies show that non-negligible fraction of spiral galaxies has nuclear rings which are rich in gas and young massive stars (Maoz et al. 1996; Carollo et al. 1998; Perez-Ramirez 2000). Since the pioneering works on the formation of nuclear ring by Schwarz (1981; 1984), it has been generally accepted that nuclear rings form from the disk materials that are transported to the central regions of galaxies due to non-axisymmetric potentials (Combes & Gerin 1985; Barth et al. 1995; Piner et al. 1995).

It has been thought that the inflowing gas is accumulated in the regions around nuclei of galaxies due to orbit crowding when there is at least one ILR (Schwarz 1981; Combes & Gerin 1985). However, detailed analyses of nuclear rings based on sticky particle simulations (Shaw et al. 1993) and hydrodynamic simulations (Piner et al. 1995; Ann & Lee 2000) show that the presence of two ILRs is requisite for the formation of nuclear rings.

Nuclear rings are observed to be round or elongated with their orientations parallel, perpendicular or at intermediate angles with the bar, with a preferential incidence of misaligned nuclear rings (Buta & Crocker 1993). If we consider that most of nuclear rings are observed in early-type barred spiral galaxies (Buta & Crocker 1993), the preponderance of misaligned nuclear rings can be understood in terms of orbital behavior of gas and stars near ILRs. In galaxies with highly concentrated mass distribution, ILRs are likely to exist and the main family of orbits is the x2 family which is perpendicular to the bar axis. But, the mechanism for aligned nuclear rings is not well understood yet.

In this work, we present some results of on-going SPH simulations for the evolution of nuclear rings in barred galaxies. In the next section, we describe the numerical methods and the model galaxies briefly. We present the results in Section III and the conclusions

are followed in the last section.

II. NUMERICAL METHODS AND MODELS

(a) Numerical Methods

The present simulations are basically the same as those of Ann & Lee (2000), but here we focus on the evolution of nuclear ring morphology. We assumed homogeneous and isothermal (10,000K) gaseous disk and introduced the bar component slowly in 0.5 bar rotation period. The number of SPH particles is about 20,000 and the initial spatial resolution is about 130 pc. We have used artificial viscosity following Hernquist & Katz (1989) with $\alpha = 0.5$ and $\beta = 1$. Although the code we are using is a fully three-dimensional one (Monaghan 1992), we have confined the distribution of particles in the disk so that we could achieve better resolution. We neglect the self-gravity of gas for most cases. The simulations are carried out up to 10 bar rotation periods.

(b) Mass Models

We adopt simple analytic potentials for model galaxies which are defined by mass fractions and scale lengths. We have used the following units to express the physical parameters of model galaxies :

Mass: $4 \times 10^{10} M_{\odot}$

Lengths: 5 kpc

Time(τ_{dyn})= 2.63×10^7 yr

Angular Speed: 37.2 km/s/kpc

The lengths of bars are fixed as 6 kpc by assuming $R_{CR} \approx 1.2a$ where R_{CR} and a are the corotation radius and the semi-major axis length of bar, respectively, except for models whose pattern speeds are high enough to avoid the ILRs. Thus, our models are defined by the the pattern speed and axial ratio of bar as well as the mass fractions and scale lengths of the four components, bulge, disk, bar, and dark halo. The model galaxies are broadly divided into two groups; type A

for the early type galaxies and type B for the intermediate type galaxies, respectively. The early type galaxies are assumed to have comparable mass fractions in the bulge and disk components, while the intermediate type galaxies are assumed to have larger mass fractions in the disk component.

Ann & Lee (2000) conducted extensive simulations with a wide range of physical parameters to analyze the response of the gaseous disks to the imposed bar potentials. The present models (A4, A5, B2, B4) are a subset of the simulations that shows representative nuclear ring morphology which is supposed to be observed in real galaxies with massive bars ($M_{\text{bar}}/M \gtrsim 0.2$). Because the presence of two ILRs is a necessary condition for the formation of nuclear rings (Ann & Lee 2000), the selected models, of course, have two ILRs. Table 1 lists the physical parameters which characterize the dynamical properties of each model. The length scales of the disk, bulge, and dark halo components are the same for all the models in Table 1, *i.e.*, $R_d = 0.6$, $R_b = 0.1$, and $R_h = 3.0$, respectively.

III. RESULTS

(a) Nuclear Morphology

Fig. 1 shows snapshots of the distribution of SPH particles of the models listed in Table 1. All the models show development of nuclear rings between the two ILRs with global spiral arms in the outer disks. The formation of nuclear rings is due to the existence of strong ILRs which induce orbit crowding near ILRs. As shown in Fig. 1, the nuclear rings of three models (A4, A5, and B4) align perpendicular to the bars which lie horizontally in Fig. 1. The nuclear ring of B2 model is smaller than others and aligns parallel to the bar axis. The morphological difference is due to the different relative strength of the bar potentials. Among models, B2 model has the strongest bar and B4 model has the weakest bar, respectively.

There are some differences in the distribution of SPH particles inside and outside the nuclear rings. As shown in Fig.1, there seem to be nuclear spirals inside the nuclear rings of the two models A4 and B4 which have

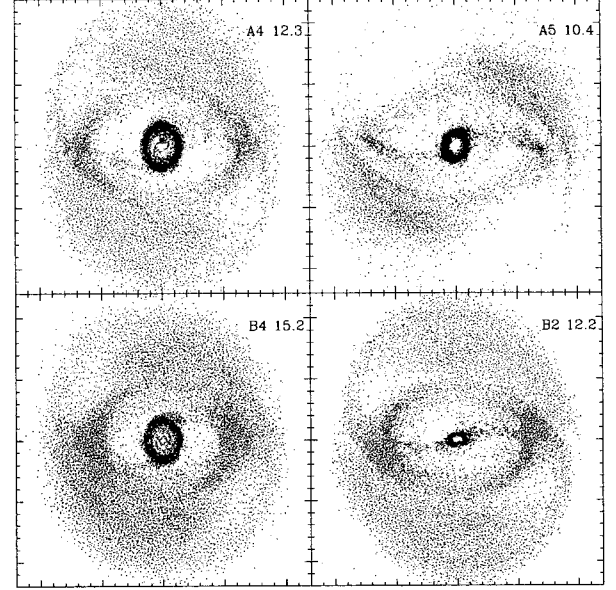


Fig. 1.— Snapshots of the distribution of SPH particles in the frame corotating with the bar. The models A4 and A5 have comparable mass fractions for disk and bulge components, while B2 and B4 models have massive disks. All the models show nuclear rings between the two ILRs. The numbers in the upper left corner of each box represent the evolution times in the unit of τ_{dyn} . The size of box is 12 kpc in one dimension. The bar lies horizontally

relatively weak bars. The nuclear spiral of A4 model is a two-armed spiral while that of B4 model shows multiple arms. There is a clear evidence of density enhancements along the leading edges of the bars, which resemble the dust lanes in barred galaxies. These dust lanes are smoothly connected to the nuclear rings.

(b) Evolution of Nuclear Rings

Fig. 2 shows the evolution of the nuclear regions of the four models. There seems to be little evolution in the relatively weak bar models, A4 and B4. The most pronounced evolution is observed in B2 model, which leads to the shrinking and fragmentation of the ring. This kind of evolution is anticipated in galaxies with strong bars (Ann & Lee 2000). The nuclear ring of NGC 4314 is a prototypical example (Ann, 2001). It is worth to note that there is a significant inflow of gas into the nucleus of the B2 model.

(c) Velocity Field and Shock Locations

Fig.3 shows snapshots of the velocity fields of highly shocked particles. By comparing the distribution of the SPH particles in Fig. 1 and the velocity fields in Fig. 3, it can be found that the nuclear rings and dust lanes are mostly made of highly shocked particles. Thus, the nuclear rings consist of the SPH particles whose orbits are changed from the x1 orbits to the x2 orbits through the

Table 1. Model parameters

| Model | a^1 | b^1 | Ω_p^2 | D^3 | B^3 | Ba^3 |
|-------|-------|-------|--------------|-------|-------|--------|
| A4 | 0.6 | 0.2 | 1.25 | .39 | .40 | .20 |
| A5 | 0.6 | 0.2 | 1.20 | .34 | .35 | .30 |
| B2 | 0.6 | 0.2 | 1.20 | .52 | .27 | .20 |
| B4 | 0.6 | 0.3 | 1.20 | .52 | .27 | .20 |

¹ a and b are the major and minor axis length of bar.

² Ω_p is the pattern speed of bar.

³ D, B, Ba are the mass fractions of disk, bulge and bar, respectively.

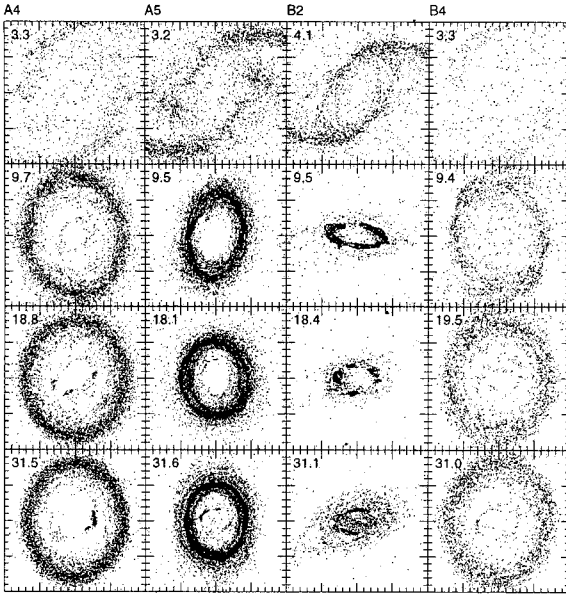


Fig. 2.— Evolution of the gaseous disks in the nuclear regions. The model with strongest bar potential (B2) shows the development of highly elongated nuclear ring. The numbers in the upper left corner of each box represent the evolution times in the unit of τ_{dyn} . The size of box is 1 kpc in one dimension. The bar lies horizontally

shocks. This is the reason why nuclear rings which are developed near the strong ILRs are aligned perpendicular to the bar unless the non-axisymmetric potential induced by the bar is strong enough to allow x1 orbits near the ILRs.

IV. CONCLUSIONS

In the presence of two ILRs, the formation of nuclear ring is a natural consequence of the bar-induced gas inflow. Shock dissipation plays a critical role for the gas to be accumulated near the ILRs. The morphology of nuclear rings depends on the dynamical properties of galaxies of which the relative strength of bar potential is the most important parameter. The relative strength of bar potentials depends on the bar parameters as well as the central mass concentration which is mainly determined by the bulge scale length.

Nuclear rings form between the two ILRs. The main family of orbits which consists of nuclear rings is x1 family of orbits. Large nuclear rings are formed in galaxies with weak bar potentials, while small nuclear rings are formed under strong bar potentials. Nuclear rings are aligned perpendicular to the bar unless the bar potentials are strong enough to allow the x1 orbits near the ILRs.

ACKNOWLEDGEMENTS

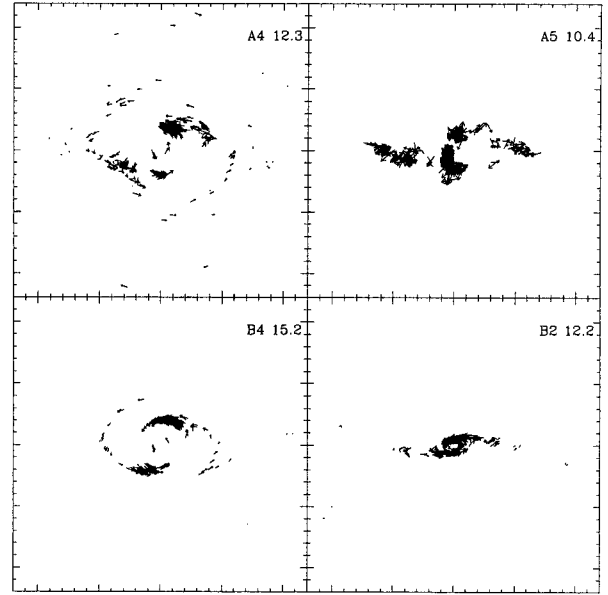


Fig. 3.— Snap shots of the velocity fields in the frame corotating with the bar. The velocity fields are plotted for the shocked gas particles only. The numbers in the upper right corner of each diagram is the evolution time in the unit of τ_{dyn} . The size of box is 12 kpc in one-dimension

This work was supported by grant No. R01-1999-00023 from the Korea Science & Engineering Foundation.

REFERENCES

- Ann, H. B. 2001, AJ, 2001
- Ann, H. B., & Lee, H. M. 2000, JKAS, 33, 1
- Barth, A. J., Ho, L. C., Filippenko, A. V., Sargent, W. L. 1995, AJ, 110, 1009
- Buta, R., & Crocker, D. A. 1993, AJ, 105, 1344
- Carollo, C. M., Stiavelli, M., & Mack, J. 1998, AJ, 116, 68
- Combes, F. & Gerin, M. 1985, A&A, 150, 327
- Hernquist, L., & Katz, N. 1989, ApJS, 70, 419
- Maoz, D., Barth, A. J., Sternberg, A., Filippenko, A. V., Ho, L. C., Macchetto, F. D., Rix, H.-W., & Schneider, D. P. 1996, AJ, 111, 2248
- Monaghan, J. J. 1992, ARA&A, 30, 543
- Prez-Ramirez, D., Knapen, J. H., Peletier, R. F., Laine, S., Doyon, R., & Nadeau, D. 2000, MNRAS, 317, 234
- Piner, B. G., Stone, J. M., & Teuben, P. J. 1995, ApJ, 449, 508
- Schwarz, M. P. 1981, ApJ, 247, 77
- Schwarz, M. P. 1984, MNRAS, 209, 93